THE BELL SYSTEM TECHNICAL JOURNAL
Vol. 59, No. 5, May–June 1980
Printed in U.S.A.

Time- and Frequency-Domain Representation of Multipath Fading on Line-of-Sight Microwave Paths

By W. D. RUMMLER

(Manuscript received December 17, 1979)

Propagation on a radio path experiencing multipath fading can be modeled in the time domain by an N-path transmission network with each path characterized by gain and delay. We examine the interrelations of such a representation with the more frequently observed frequency domain characteristics of the channel. We show that the decibel gain and envelope delay distortion of the transfer function may both be expressed as summations of elementary functions each associated with a zero in the complex frequency domain. We find that the average frequency spacing of the zeros, and of transmission minima, is determined by the maximum delay. Although published propagation data indicate an average spacing of 100 MHz or more for common carrier radio hops, we verify that closely spaced zeros can occur with nominal path gains and short delay spreads. This is demonstrated by developing multipath synthesis procedures which allow path gains and delays to be determined from a specification of gain and/or delay distortion in a finite frequency band. The resulting networks are not unique; for instance, more than 5000 three-path delay networks with delay spread less than 10 ns can be found to provide a match over a 60-MHz band near 6 GHz to a sample gain shape with two minima. These developments provide the basis for a qualitative comparison of the ability of a channel modeling function to statistically represent the state of the transmission channel. We describe the limitations of both delay and complex power series models of varying degrees of complexity.

I. INTRODUCTION

The use of digital radio in the common carrier, line-of-sight, microwave radio bands has rekindled an interest in propagation modeling.[1–4] Recently, a statistical model was developed[4,5] for a 26.4-mile path in

the 6-GHz band (30-MHz bandwidth) at Palmetto, Georgia, using a multipath channel model. It was found, in the modeling study,[4] that for appreciable periods of time the channel was well characterized with modeled delay spreads exceeding 25 ns. Such a spread is considerably larger than the 8.5 ns that would be predicted on the basis of (deterministic) ray modeling,[6] or expected on the basis of previous propagation studies.[7-9] One of the objectives of the present study is to verify that these results are not inconsistent for multipath (three or more paths) channels.

The analysis provides the basis for determining the extent to which one can predict the transmission characteristics in a narrowband (20- to 40-MHz bandwidth) channel from knowledge of the physical delays present in the radio path and, conversely, the extent to which one can determine the physical delays present in this path from observation of the channel. These developments clarify the limitations of existing statistical models for channel characterization in the frequency domain and indicate directions for developing extended models.

While a number of authors have placed bounds on the attenuation and group delay produced by finite-delay-spread channels,[3,10,11] the present work is the first attempt to describe the overall structure of the frequency response of a multipath channel. Our approach is to view the channel transmission characteristic from the standpoint of classical network theory. We begin in Section II by reviewing the properties of network transfer functions and developing simple means for calculating the channel attenuation and envelope delay distortion (or group delay). The frequency dependence of the envelope delay distortion and the channel attenuation provide a complete description of a transfer function. These quantities are simply related to the complex frequency (s-plane) representation of the transfer function. The transmission path is modeled as an ideal N-path network, which provides at the receiver N scaled replicas of the transmitted signal, where each replica appears at a discrete delay. The transfer function of such a network can be uniquely represented by its s-plane zeros. Such a canonic representation is useful because it allows one to obtain the envelope delay and attenuation characteristics from the zero configuration. Considerable attention is given to determining the position and distribution of zeros from a given multipath transfer function (MTF).

The procedure is inverted in Section III, where we develop techniques for synthesizing MTFs from specified s-plane zeros. The insights provided are used in Section IV to compare simple multipath and power series models that are appropriate for statistical modeling of narrowband radio channels. A summary of results and conclusions is given in the final section.

II. DISCRETE MULTIPATH TRANSFER FUNCTIONS

2.1 Characterizing network transfer functions

The transfer properties of a network may be characterized by $H(s)$, the complex voltage transfer function in the s-plane, or complex-frequency plane. If we represent the effective voltage at the input (transmitting antenna) by

$$V_T(s) = e^{st}, \tag{1}$$

where s is the complex frequency,

$$s = \sigma + j\omega, \tag{2}$$

then the effective voltage at the output (receiving antenna) is given by

$$V_R(s) = H(s)V_T(s). \tag{3}$$

We take eq. (3) as the definition of the transfer function of the propagation path. As the transfer function of a passive network, $H(s)$ must be analytic in the right half plane[12] ($\sigma > 0$). Hence, it may have poles only in the left half plane but zeros anywhere. If all the zeros are in the left half plane, the function is described as a minimum phase function; otherwise, it is nonminimum phase.

A transfer function may be completely specified by its attenuation (or loss) and phase functions on the $j\omega$-axis.[13] We may define these functions by writing

$$H(j\omega) = e^{-(\alpha + j\beta)}, \tag{4}$$

where $\alpha(\omega)$ and $\beta(\omega)$ are the loss function in nepers and the phase-lag function in radians, respectively. We shall use two closely related, but equivalent, functions to describe the transfer impedance: $A(\omega)$, the attenuation in decibels; and $D(\omega)$, the delay distortion function, where

$$A(\omega) = -20 \log|H(j\omega)| = \left(\frac{20}{\ln 10}\right)\alpha(\omega) \tag{5}$$

and

$$D(\omega) = \frac{\partial\beta}{\partial\omega}. \tag{6}$$

The delay distortion function is also referred to as the envelope delay distortion function, the group delay function, or simply the delay function, when the meaning is not ambiguous.

To obtain a more explicit expression for the delay distortion function, we write

$$H(s) = R(\sigma, \omega) + jX(\sigma, \omega). \tag{7}$$

Comparing (4) and (7), we see that

$$\beta = -\text{arc tangent} \frac{X}{R}\bigg|_{\sigma=0}. \tag{8}$$

Hence from (6) and (8),

$$D(\omega) = \frac{X(\partial R/\partial\omega) - R(\partial X/\partial\omega)}{X^2 + R^2}\bigg|_{\sigma=0}. \tag{9}$$

Applying the Cauchy-Riemann conditions, we obtain

$$D(\omega) = -\frac{\partial}{\partial\sigma} \ln|H(s)|\bigg|_{\sigma=0}. \tag{10}$$

In addition to its utility in deriving the delay distortion function from the transfer function, the expression in eq. (10) is particularly useful for qualitatively visualizing the shape of a delay distortion function given the pole-zero distribution of the transfer function. One merely visualizes $|H(s)|$ as the height above the s-plane of a uniform infinitely stretchable sheet pushed infinitely high at the poles and to zero height at the zeros of $H(s)$. The delay distortion is the negative of the (logarithmic) slope of the surface in the σ-direction at the $j\omega$-axis.

2.2 Characterization of multipath transfer functions

Consider a propagation link characterized by N discrete paths. If the signal replica arriving via the nth path has amplitude a_n and delay τ_n, we may write the transfer function for the propagation link from eq. (3) as

$$H(s) = \sum_{n=1}^{N} a_n e^{-s\tau_n}. \tag{11}$$

We number the paths in order of increasing delay and, for simplicity, take the delay of the first path as zero. That is, we subtract the delay of the first path from all physical path delays. Hence,

$$0 = \tau_1 < \tau_2 < \tau_3 < \cdots < \tau_N. \tag{12}$$

Since $H(s)$ is analytic and of bounded magnitude in the finite s-plane, it is classified as an integral or entire function. As such, it can be expanded in terms of its zeros as an infinite product:[14]

$$H(s) = H(0)\{e^{[sH'(0)/H(0)]}\} \prod_{k=1}^{\infty} \left(1 - \frac{s}{s_k}\right) e^{s/s_k}. \tag{13}$$

It is assumed that the zeros have been numbered in some consistent manner and that each zero appears as often as is required by its degree

of multiplicity. The coefficient of s in the leading exponential term may be determined from eq. (11) as

$$\frac{H'(0)}{H(0)} = -\frac{\sum_{n=1}^{N} \tau_n a_n}{\sum_{n=1}^{N} a_n}. \tag{14}$$

Hence, the leading exponential term represents the weighted average delay of the paths of the network.

The infinite product representation of (13) provides a basis for describing the properties of $H(s)$. The representation may be shown to be uniformly and absolutely convergent in the finite s-plane,[15] and each of the factors in the product is referred to as a primary factor. It is instructive to examine the kth primary factor,

$$F_k(s) = \left(1 - \frac{s}{s_k}\right) e^{s/s_k}, \tag{15}$$

where

$$s_k = \sigma_k + j\omega_k \tag{16}$$

denotes the location of the kth zero. The location of a zero is unrestricted, except that we allow $j\omega$-axis zeros only as a limiting case ($\sigma_k \to 0$). The contribution of the primary factor to the channel attenuation may be obtained with eq. (5) as

$$A_k(\omega) = -10 \log \frac{\sigma_k^2 + (\omega - \omega_k)^2}{\sigma_k^2 + \omega_k^2} - (20 \log e) \frac{\omega\omega_k}{\sigma_k^2 + \omega_k^2}. \tag{17}$$

For physical networks, the zeros always occur in conjugate pairs. Hence, there is a zero at $(\sigma_k, -j\omega_k)$, which produces a frequency term that cancels the last term in eq. (17). Thus, we may represent $A_k(\omega)$ by

$$A_k(\omega) = -10 \log \frac{\sigma_k^2 + (\omega - \omega_k)^2}{\sigma_k^2 + \omega_k^2}. \tag{17a}$$

The delay distortion corresponding to F_k is obtained with eq. (10) as

$$D_k(\omega) = \frac{\sigma_k}{\sigma_k^2 + (\omega - \omega_k)^2} - \frac{\sigma_k}{\sigma_k^2 + \omega_k^2}. \tag{18}$$

From eqs. (5), (10), and (13) to (18), it is apparent that the attenuation and delay functions of the transfer function can be expressed, respectively, as

$$A(\omega) = -20 \log H(0) + \sum_{k=1}^{\infty} A_k(\omega) \tag{19}$$

and

$$D(\omega) = -\left(\frac{H'(0)}{H(0)}\right) + \sum_{k=1}^{\infty} D_k(\omega). \tag{20}$$

Thus, the channel attenuation and delay functions can be expressed as the summation of primary attenuation and delay distortion functions.

The function $A_k(\omega)$ is similar to the response of a resonant circuit. Using the standard notion for tuned circuits, we let

$$f_{bk} = \frac{|\sigma_k|}{\pi}$$

$$Q_k = \frac{\omega_k}{2|\sigma_k|} = \frac{f_k}{f_{bk}}$$

$$\delta_k = \frac{f - f_k}{f_{bk}} = Q_k \frac{f - f_k}{f_k}, \tag{21}$$

where f_{bk} is the 3-dB bandwidth of the response, Q_k is the equivalent circuit Q or the ratio of the resonant frequency to the bandwidth, and δ_k is the frequency variable measured in 3-dB bandwidths from resonance. Using eqs. (21) in (17a) and (19), we find

$$A_k(\omega) = 10 \log(1 + 4Q_k^2) - 10 \log[1 + (2\delta_k)^2] \tag{22}$$

$$D_k(\omega) = \frac{1/\sigma_k}{1 + (2\delta_k)^2} - \frac{1/\sigma_k}{1 + 4Q_k^2}. \tag{23}$$

These two expressions both involve the frequency variable through the term $1 + 4\delta_k^2$: the delay distortion function varies inversely with this term; the attenuation depends on its logarithm. Equations (22) and (23) are plotted in Fig. 1. The attenuation displays a maximum at the resonant frequency ($\delta_k = 0$). The delay distortion function is more strongly peaked and localized than the logarithmically varying attenuation curve. Note that, for $\sigma_k < 0$, corresponding to a minimum phase zero, the delay function has a minimum at the resonant frequency, whereas for $\sigma_k > 0$, corresponding to a nonminimum phase zero, the delay function has a maximum. This difference is normalized out of Fig. 1.

One may visualize the attenuation function of $H(s)$ as the resultant of a summation of curves such as that shown in Fig. 1, with each curve in the summation being translated and scaled (compressed or expanded) in frequency to correspond to the position of the associated complex zero. The delay distortion function may be visualized as a similar type of summation. Thus, the attenuation and delay in a band of frequencies will be dominated by the zeros that are "close" to the band. Zeros with f_k within the band will tend to produce maxima in

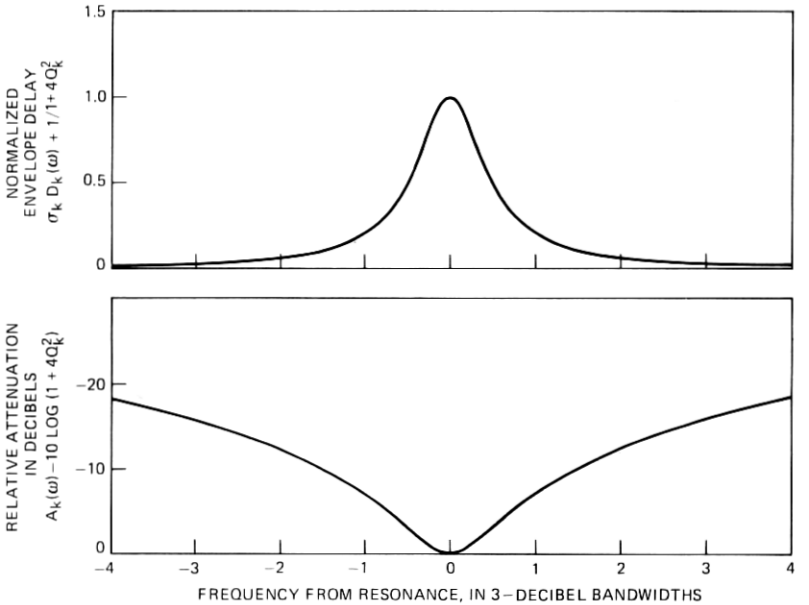

Fig. 1—Attenuation and delay of primary functions.

the attenuation and either minima or maxima in the delay. Zeros with f_k outside the band are evidenced in the in-band attenuation by an attenuation slope; the slope observed would be the net slope resulting from all zeros. While one can make a similar observation with respect to delay, it is apparent that the effects of distant zeros are more pronounced in the attenuation than in the delay. That is, the attenuation characteristic of a primary factor decreases much more slowly with frequency than does the envelope delay. The interested reader may verify these statements by examining the asymptotic behavior of $A_k(\omega)$ and $D_k(\omega)$; however, rather than pursue the matter further here, we shall demonstrate this effect with examples in Section III.

2.3 Determining transfer function zeros

In the preceding section, we showed how the attenuation and delay distortion of a multipath transfer function are related to its s-plane zeros. In this section, we show by a conceptual example how to obtain the s-plane zeros from the MTF. Although the precise calculation of the positions of the zeros is a formidable problem, it is relatively simple to determine their average density of occurrence. To this end, we shall assume that all the multipath delays are expressible as rational numbers.* While this is a trivial limitation from a physical standpoint,

* Or contain a common irrational factor.

since we cannot determine the rationality of a physical quantity from finite measurement, it greatly simplifies the mathematical development.*

If each of the delays in eq. (11) is rational, it is possible to find a pair of relatively prime integers p_n and q_n for each τ_n such that

$$\tau_n = \frac{p_n}{q_n}. \tag{24}$$

Defining a delay, τ_0, by

$$\tau_0 \equiv 1/\text{lcm}\{q_n\}, \tag{25}$$

where $\text{lcm}\{q_n\}$ denotes the least common multiple of the q_n's; and integers, m_n, by

$$m_n \equiv \frac{p_n}{q_n} \text{lcm}\{q_n\}, \tag{26}$$

we may write (11) as

$$H(s) = \sum_{n=1}^{N} a_n e^{-m_n s \tau_0}. \tag{27}$$

It is apparent that $H(s)$ is a periodic function with a period along the frequency axis of $f_p = 1/\tau_0$. That is,

$$H(s + j2\pi f_p) = H(s). \tag{28}$$

If we now make the transformation

$$z = e^{-s\tau_0} \tag{29}$$

in (27), we obtain the polynomial $P(z)$ where

$$P(z) = H\left(\frac{-\ln z}{\tau_0}\right) = \sum_{n=1}^{N} a_n z^{m_n}. \tag{30}$$

Since the order of the polynomial, $P(z)$, is m_N, it can be factored in terms of its roots. Denoting the qth root by z_q, we have

$$P(z) = a_1 \prod_{q=1}^{m_N} \left(1 - \frac{z}{z_q}\right), \tag{31}$$

where multiple roots are multiply reported. We note that for real coefficients, a_n, the roots will be real or in complex conjugate pairs.

---

* It is worth noting that, with irrational delays, $H(s)$ would become an almost periodic function (with infinite N allowed as long as $\Sigma \mid a_n \mid$ is finite) (Ref. 16); with rational delays and infinite N, the function $H(s)$ would become a limit periodic function, a subset of almost periodic functions (Ref. 17). While the developments of the preceding section are valid for almost periodic functions, the results of this section are strictly true only for a finite number of rational delays. These results can be extended in a limiting sense to the more general classes of multipath transfer functions if they are restricted to have a bounded set of delays (Ref. 18); however, the mathematical complexity required would mask the simplicity of the results.

We see that there are m_N roots in the z-plane. Since a sheet of the z-plane transforms, by eq. (29) into the s-plane as a strip of infinite extent in σ and extent $2\pi/\tau_0$ along the $j\omega$-axis, we conclude that there are $m_N\tau_0$ zeros per hertz along the $j\omega$-axis. Since $m_N\tau_0$ is the maximum delay present in $H(s)$, the average spacing between zeros is $1/\tau_N$ Hz. Because delays are measured relative to the delay of the first path, the average spacing between zeros (in hertz) is equal to the reciprocal of the spread of delays present in the propagation path. We return to this point in the next section.

Transforming $P(z)$, as given by eq. (31) back into the s-plane, we have

$$H(s) = P(e^{-s\tau_0}) = a_1 \prod_{q=1}^{m_N} \left(1 - \frac{1}{z_q} e^{-s\tau_0}\right). \tag{32}$$

However, each of the factors in eq. (32) may be represented as an infinite product. Thus we obtain, after manipulation,

$$H(s) = H(0)e^{[sH'(0)/H(0)]} \prod_{q=1}^{m_N} \prod_{p=-\infty}^{\infty} \left(1 - \frac{s}{s_{qp}}\right) e^{s/s_{qp}}, \tag{33}$$

where

$$s_{qp} = \frac{-1}{\tau_0} [\ln r_q + j(\theta_q + 2\pi p)] \tag{34}$$

and

$$z_q = r_q e^{j\theta_q}. \tag{35}$$

The expansion of (33) is identical to that of (13) if one develops a numbering scheme that relates a given s_{qp} to a unique s_k. For instance,

$$s_k = s_{qp} \tag{36}$$

for

$$\begin{aligned} k &= q + (2p - 1)m_N \qquad p > 0 \\ &= q - 2pm_N \qquad p \leq 0. \end{aligned} \tag{37}$$

Thus we have developed the means of relating the delay representation and the product representation of a multiple delay function. Before we put this knowledge to use in Section III, synthesizing delay networks from s-plane zero configurations, we shall pursue the topic of the distribution of zeros in the following subsection.

2.4 Estimation of channel delay spread

In Section 2.3, we demonstrated that, for a time-invariant channel, the total spread of delays in the channel, τ_N, is equal to the average

number of zeros per unit frequency along the $j\omega$-axis. In this subsection, we argue that for a propagation link one can estimate, from amplitude observations in a narrow-frequency band, the average value of the total spread of channel delays giving rise to frequency selective attenuation in the channel.

Let us assume that we have a microwave radio channel characterized by a multipath transfer function as given by eq. (11) except that the amplitudes and delays are random processes evolving continuously in time but slowly with respect to the rate at which we can probe the channel. Since the amplitudes and delays are physical quantities, they can be represented by continuous and bounded functions of time. (Short pulse observations[7] indicate that the atmosphere has a limited capability of increasing the a_n's through focusing; observation[7] and modeling[6] do not indicate a mechanism for providing relatively unattenuated delays much in excess of 10 ns for paths on the order of 25 miles long.)

Let us first assume that the statistics of the model are stationary and that as time evolves we can, by some means, observe all the zeros in a strip of the s-plane extending from a frequency f_1 to a frequency f_2. If $n_a(f_1, f_2, t)$ is the number of zeros in the strip at time t, the average delay spread would be estimated as

$$\overline{\tau_N(f_1, f_2)} = \lim_{T\to\infty} \frac{1}{2T} \int_{-T}^{T} \frac{n_a(f_1, f_2, t)}{(f_2 - f_1)}\, dt, \tag{38a}$$

or in discrete time form as

$$\overline{\tau_N(f_1, f_2)} = \lim_{M\to\infty} \frac{1}{2M} \sum_{p=-M}^{M} \frac{n_a(f_1, f_2, p\Delta t)}{(f_2 - f_1)}. \tag{38b}$$

the expressions in (38a) and (38b) are equivalent as long as the spacing, Δt, between time samples is sufficiently small.

From eqs. (17) and (19), we know that each s-plane zero (ω_k, σ_k) can be evidenced by an attenuation maximum (transmission minimum) at $\omega = \omega_k$. However, if σ_k is too large, its presence may be masked by a local slope in attenuation; i.e., there may be no maximum.* Therefore, the number of maxima of $A(\omega)$ in an observed frequency band, which we denote by $n_0(f_1, f_2, t)$ is less than or equal to the number of zeros present in the strip, or

$$n_0(f_1, f_2, t) \leq n_a(f_1, f_2, t). \tag{39}$$

* There are no strong statements to be made concerning the distribution of zeros in the σ-dimension. For multipath transfer functions with $\sum |a_n|$ finite and bounded delay, one can prove that all zeros lie in a strip of finite width parallel to the frequency axis (Ref. 18).

Since a well-designed microwave radio path does not show a preference for fading at any particular frequency, the choice of the frequencies f_1 and f_2 is not important as long as the frequency interval (f_1, f_2) is large enough that a reasonable number of events ($n_0 > 0$) are observed in a manageable time period.

In characterizing multipath fading, the statistical picture is further complicated because fading is a nonstationary process; fading occurs during discrete time periods when the atmospheric conditions are appropriate. Thus, to statistically characterize multipath propagation, one assumes that multipath time periods are identifiable and that the statistics are always the same in each of these periods. On this basis, we would estimate $\hat{\tau}_N$, the average value of the maximum delay spread, as

$$\hat{\tau}_N(f_1, f_2) = \frac{\int_{\text{multipath}} n_0(f_1, f_2, t)\, dt}{(f_2 - f_1) \int_{\text{multipath}} dt}, \tag{40a}$$

or with discrete time samples as

$$\hat{\tau}_N(f_1, f_2) = \frac{\sum_{\{i_m\}} n_0(f_1, f_2, it)}{(f_2 - f_1) \sum_{\{i_m\}} 1}, \tag{40b}$$

where $\{i_m\}$ denotes the set of time indices covering the periods during which multipath fading occurred.

The estimator of (40b) was implemented for data acquired at 6 GHz on a 26.4-mile path near Atlanta, Georgia, in 1977. The estimated delay[4] was 9.1 ns using the study multipath time. Using subsets of the fading intervals chosen on the basis of fade depth and shape gave estimated values of $\hat{\tau}_N$ between 6 and 11 ns. This consistency implies that the assumption of statistical homogeneity was a reasonable one for the data studied. The 9.1 ns is consistent with the maximum values of 7 ns observed[7] with short pulse measurements on a 22.8-mile path at 4 GHz,* and with predictions of maximum delays of 8.5 ns based on a three-layer propagation model.[6] The estimator of (40b) may be applied to published broadband spectral measurements. A delay of 6 ns is obtained from measurements on the 22.8-mile path,[8] and 9 ns is obtained from measurements at 4 GHz on a 31-mile path in Ohio.[9]

The above results suggest that it may be reasonable to model

* The short pulse measurements were performed with a linear received voltage scale and a limited maximum delay measuring capability. They do not preclude the existence of small-amplitude delayed components, particularly at large delays.

wideband multipath-fading channel transfer characteristics by applying a distribution for the number and location of the zeros of the functions. For instance, one could assume that the distribution of zeros along the frequency ($j\omega$) axis is Poisson, and that the distribution of the σ coordinates of position are identical, but independent for each zero. The state of the channel would be determined by a Monte Carlo selection. Such a model does not appear to be inconsistent with the observations above; however, its verification and parameterization would require considerable effort.

2.4.1 Effects of very large delays

As may be observed from eqs. (38) to (40), the delay spread, $\hat{\tau}_N$, estimated from amplitude information is biased towards low values. This bias is due to the limited precision in measuring the attenuation spectrum. To show that this masking can be significant in a case of interest, consider the case where the multipath transfer function, $H(s)$, contains two parts: one due to multipath propagation $H_p(s)$ and another due to multipath reflections in the receiving waveguide runs, $H_w(s)$. That is,

$$H(s) = H_p(s)H_w(s). \tag{41}$$

Assume a single delayed return due to mismatch or mode conversion at both ends of a waveguide run. Then

$$H_w(s) = 1 - b_w e^{-s\tau_w}, \tag{42}$$

where τ_w is the round-trip delay associated with the waveguide. We assume for τ_w a typical value of 400 ns. Using eqs. (5) and (10), the attenuation and delay produced by $H_w(s)$ may be written as

$$A_w(\omega) = -10 \log(1 + b_w^2 - 2b_w \cos \omega\tau_w) \tag{43}$$

$$D_w(\omega) = \frac{b_w\tau_w(b_w - \cos \omega\tau_w)}{1 + b_w^2 - 2b_w \cos \omega\tau_w}. \tag{44}$$

Both these functions are periodic in frequency with a period of 2.5 MHz for the given delay. The peak-to-peak variation of amplitude and delay are

$$\Delta A_w = 20 \log \frac{1 + b_w}{1 - b_w} \tag{45}$$

and

$$\Delta D_w = \frac{2b_w\tau_w}{1 - b_w^2}. \tag{46}$$

For $b = 0.01$, which corresponds to the delayed signal being 40 dB

below the primary signal,* one finds that the peak-to-peak variation in attenuation is 0.17 dB, while the peak-to-peak variation in delay is 12 ns. Hence, the effect of such a waveguide multipath would be difficult to detect from observations of attenuation. The delay distortion of 12 ns, however, would be comparable to the delay distortion produced by a rather severe fade.[19]

One may draw two conclusions from the preceding calculation. First, one must have good return loss and/or short waveguide runs to make phase coherent propagation measurements on a radio path. Second, in estimating the channel delay spread from the number of attenuation maxima, the value obtained reflects the largest delays that contribute to the attenuation selectivity and not the largest physical delay that will have any impact on the received signal. This effect may have been in evidence in Ref. 4, where large delays were estimated when an average of the type given in eq. (40) was applied to a subset of scans that had little attenuation shape in band.

III. SYNTHESIS OF MULTIPATH TRANSFER FUNCTIONS

The synthesis problem consists of finding a set of amplitudes and delays for an MTF, given the position of a finite number of zeros in a given frequency band. In Section 3.1, we briefly review synthesis from a single zero. Section 3.2 describes how to synthesize a three-path MTF from the specification of a pair of zeros. Other approaches to the two-zero problem and the M-zero problem are discussed in Section 3.3.

3.1 Synthesis from a single zero

We may synthesize an MTF for a single zero, at $s_0 = \sigma_0 + j\omega_0$, by taking a single term from the product representation of (32); thus,

$$H(s) = a[1 - be^{-(s-j\omega_0)\tau_0}], \tag{47}$$

where

$$b = e^{\sigma_0\tau_0} \tag{48}$$

and a represents the magnitude of the remaining terms at $s = s_0$. Although (47) appears to be a two-path transfer function, it cannot, in general, be synthesized by a transmission link with two real paths. (Synthesis with two real paths is possible only if $\omega_0\tau_0$ is an odd multiple of π.) Since it can be synthesized with three paths under the constraint that two of the paths have very nearly the same delay,[1] it has been described as a simple three-path model of a fade.

Figure 2 shows the location of the s-plane zeros of $H(s)$ as given by

* A value of 50 dB would be more typical of a well-designed and -installed system.

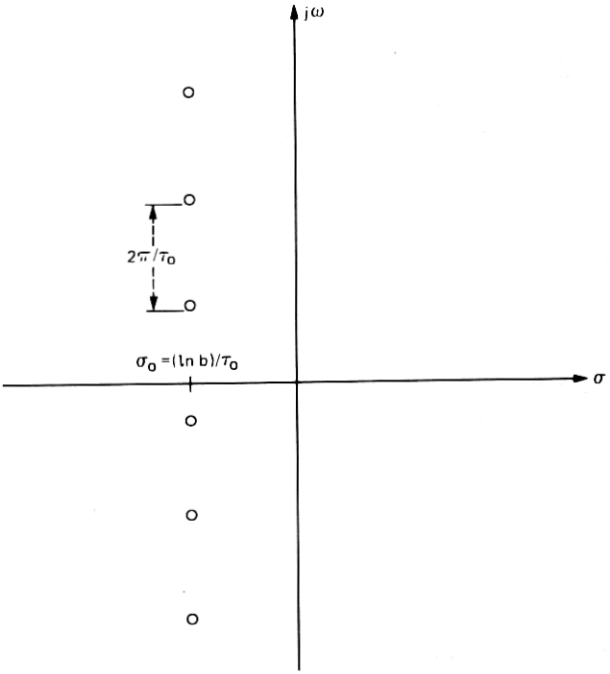

Fig. 2—Zeros of transfer function of a simple three-path fade.

(47). We note that the function is minimum-phase (all zeros in the left half plane) when $\sigma_0 < 0$ or $b < 1$; it is maximum-phase (all zeros in the right half plane) when $\sigma_0 > 0$ or $b > 1$. In a given frequency band, the attenuation and delay distortion of such a function depend only on the location of the closest zero, and are independent of τ_0 for τ_0 sufficiently small or the zero spacing sufficiently large. In particular, it is shown in the appendix that a function such as that given by (47) may be approximately matched over a bandwidth, f_B, by functions of the same form but different delay. The magnitudes of such functions match to within 0.4 dB as long as $\tau_0 < 1/(6\ f_B)$. Furthermore, the fractional difference in the delay distortion of these matched functions over the same bandwidth is less than 10 percent if, in addition, $|\sigma_0| < 0.83/\tau_0$, or $b > 0.436$. For this reason, a simple three-path fade model can be used to synthesize the effects of a single transmission zero in or near a band of frequencies.

3.2 Synthesis with three paths

Consider the problem of finding a three-path fade that will have zeros at two specified complex frequencies. Designate the locations of the zeros by $s_1 = \sigma_1 + j\omega_1$, and $s_2 = \sigma_2 + j\omega_2$, with $\omega_2 > \omega_1$. We wish to find amplitudes and delays so that

$$H(s_1) = H(s_2) = 0 \tag{49}$$

for

$$H(s) = 1 + a_2 e^{-s\tau_2} + a_3 e^{-s\tau_3}. \tag{50}$$

For convenience, we define the mid-frequency and half-separation, respectively, as

$$\begin{aligned} \omega_c &= \tfrac{1}{2}(\omega_1 + \omega_2) \\ \Delta\omega &= \tfrac{1}{2}(\omega_2 - \omega_1). \end{aligned} \tag{51}$$

At the mid-frequency, ω_c, we can represent $H(j\omega_c)$ by a phasor diagram as shown in Fig. 3. Since each phasor could have made any number of rotations in getting to the angles θ_2 and θ_3, we may write

$$\begin{aligned} \omega_c\tau_2 &= \theta_2 + 2\pi M_2 \\ \omega_c\tau_3 &= \theta_3 + 2\pi M_3, \end{aligned} \tag{52}$$

where M_2 and M_3 are integers representing the whole number of rotations, which is also equivalent to the integral number of periods at the center frequency contained in the delays. Using eqs. (50) to (52), we may write (49) explicitly as

$$\begin{aligned} 1 + a_2 e^{-j\theta_2} e^{-\sigma_1\tau_2} e^{j\Delta\omega\tau_2} + a_3 e^{-j\theta_3} e^{-\sigma_1\tau_3} e^{j\Delta\omega\tau_3} &= 0 \\ 1 + a_2 e^{-j\theta_2} e^{-\sigma_2\tau_2} e^{-j\Delta\omega\tau_2} + a_3 e^{-j\theta_3} e^{-\sigma_2\tau_3} e^{-j\Delta\omega\tau_3} &= 0. \end{aligned} \tag{53}$$

For an arbitrary choice of the integers M_2 and M_3, (52) and (53) may be solved iteratively for a self-consistent solution. One begins by assuming values for the angles θ_2 and θ_3, using (52) to determine τ_2 and τ_3, and then solving (53) for a_2, a_3, θ_2, and θ_3. When the same set of θ's or τ's is obtained in two successive iterations, the solution has converged. In cases that have been tried, to date, the procedure has converged to ten-place accuracy in one to four iterations.

The convergence is improved (usually by only one iteration) by making a good initial choice of θ_i's. One may choose wisely by observing that the complex amplitude of $H(j\omega)$ traces an epicycloidal curve as shown in Fig. 4. An epicycloid is the locus of a point on a wheel whose

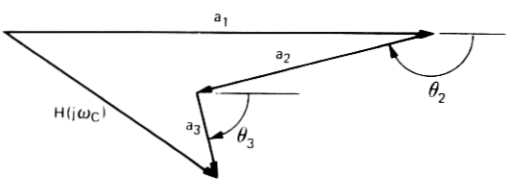

Fig. 3—Phasor diagram of three-path fade at mid-frequency, ω_c.

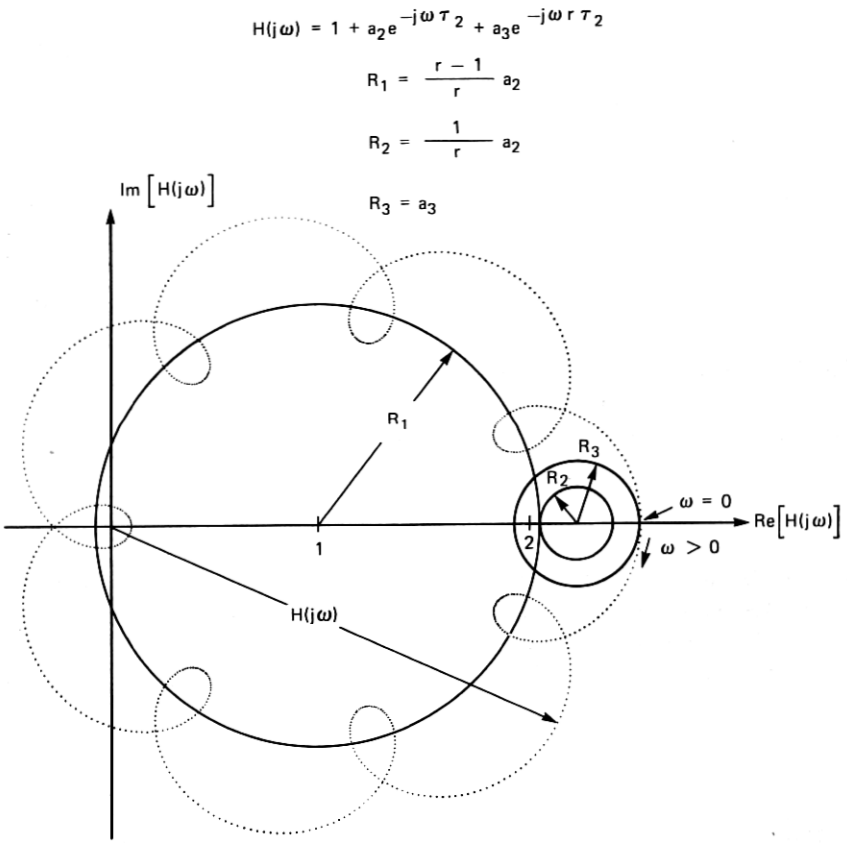

Fig. 4—Polar representation of a three-path fade for $a_2 = 1.2$, $a_3 = 0.30$ with points spaced by 1 MHz for $\tau_2 = 1.39$ ns, $r\tau_2 = 11.1$ ns.

hub is rolling on another circle. If the generating point is within the hub ($\tau_3 a_3 < \tau_2 a_2$), the locus is a prolate epicycloid; if the generating point is at a radius greater than the hub radius ($\tau_3 a_3 > \tau_2 a_2$), the curve is a curtate epicycloid. Note that the curve closes on itself in a single rotation of the wheel about the entire circle only if τ_3 is an integral multiple of τ_2, i.e., if $1/\tau_2$ is the period of $H(s)$ along the frequency axis.

One may also show that each encirclement of the origin (in a clockwise direction) corresponds to a nonminimum-phase, or right-half-plane, zero. While many additional insights can be obtained from a detailed examination of this geometric model, its primary use is in choosing initial values of θ_1 and θ_2. The most rapidly convergent starting values have generally been $\theta_2 = 180°$, $\theta_3 = 0$.

3.2.1 Examples of three path synthesis

As an example of the application of the method, consider the case where the frequency coordinates of the zeros are 5.980 and 6.020 GHz,

and $\sigma_1 = \sigma_2 = -0.0214$ nepers per nanosecond. This choice of zero locations allows a comparison between three-path fades and an observed simple three-path fade (in this case, realizable as a two-path fade) given by

$$H_2(j\omega) = 0.0116[1 + 0.5729\, e^{-j2\pi(25f)}]. \tag{54}$$

This function has zeros at the indicated locations* and parameters close to those obtained from field data.[1,4]

The attenuation and delay distortion of the MTF of (54) are compared to those of four different three-path MTFs in Fig. 5. All these MTFs have zeros at the two required complex frequencies; they were obtained by solving (52) and (53) for different values of the integers M_2 and M_3 which represent the number of periods of oscillation (⅙ ns at the center frequency) contained in τ_2 and τ_3, respectively. The parameters of the MTFs are indicated in the table on the figure. All five MTFs have virtually identical delay distortion characteristics in the frequency band shown (except for a constant delay shift). The attenuation characteristics of the MTFs, with appropriate scaling, differ from each other by less than 1 dB and from the two-path characteristic by 2 dB or less at all frequencies shown. These similarities are obtained despite the large differences in the maximum delays in the MTFs. The second MTF has a maximum delay of 2.2 ns, which is less than ⅒ that of the two-path fade.

Note that three of the four three-path MTFs in Fig. 5 have the same normalization in that the first path gain is unity. That is, the MTFs represented by curves 2, 3, and 4 were chosen from many available because they had transmission minima at the same level (near 45 dB) as the two-path fade (curve 1). If the MTF represented by curve 5 were normalized for unity gain in the first path, its minimum transmission level would be at 24.3 dB. This MTF was included to indicate the large range of transmission levels that may be obtained for three-path transfer functions with normalized path gains and prescribed zero positions which provide closely matched shapes in attenuation and delay distortion characteristics.

While the two-path fade with the prescribed zero locations is unique, it is apparent that there is a two-parameter family of three-path MTFs with these zero locations. Since each increment in M_2 or M_3 increases the delay of the corresponding path by approximately ⅙ ns [see eq. (52)], for the given pair of zero locations, one can find approximately 10,000 three-path MTFs, all of which have essentially the same attenuation and delay characteristics and maximum delay less than 25 ns.

Since the five MTFs represented in Fig. 5 have left-half-plane zeros

* For these examples, we measure delays in nanoseconds, frequencies in gigahertz, and σ in nepers per nanosecond.

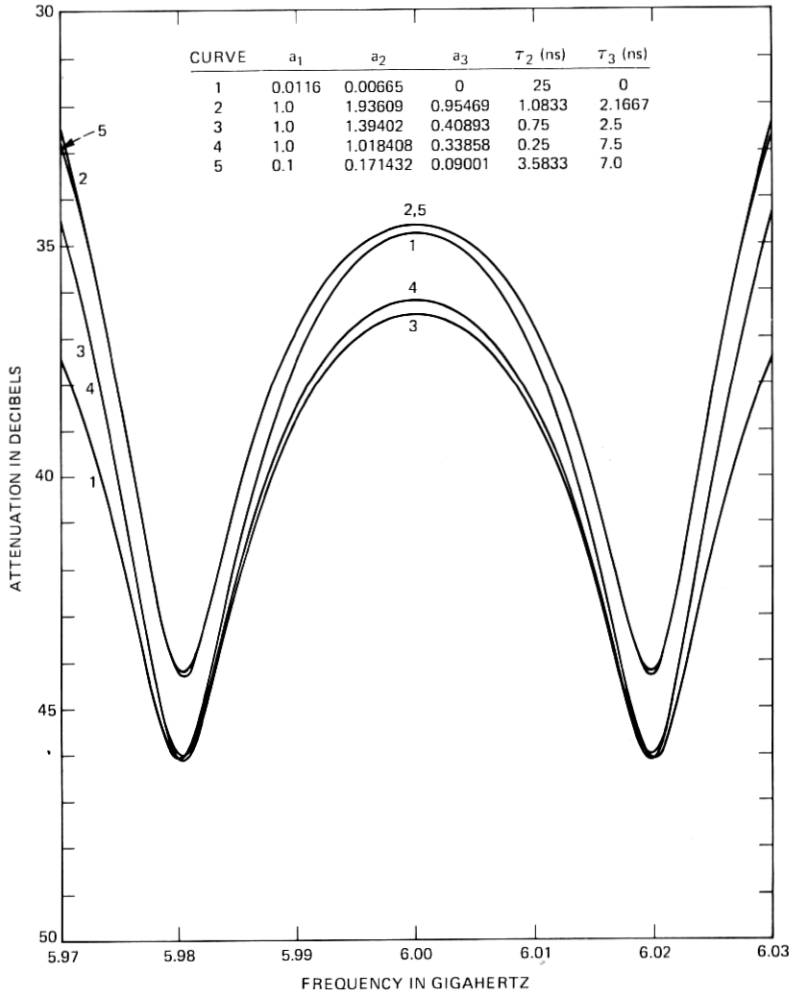

Fig. 5a—Attenuation characteristics of two-path (curve 1) and three-path MTFs with transmission minima at 5980 and 6020 MHz. The transfer function zeros associated with these minima are in the left half plane.

in the plotted band, they appear to be minimum phase functions. By comparing (54) with (47) and (48) or Fig. 2, one may verify that the two-path MTF in Fig. 5 is truly minimum phase; it has all zeros in the left half plane. Forming the z-plane polynomials for the second MTF in Fig. 5, as in eqs. (29) and (30), one may show directly that MTF No. 2 is also minimum phase. (The right half of the s-plane maps into the interior of the unit circle in the z-plane.) Using Fig. 4, one may show that the third MTF in Fig. 5 is also minimum-phase. Equations (5) and

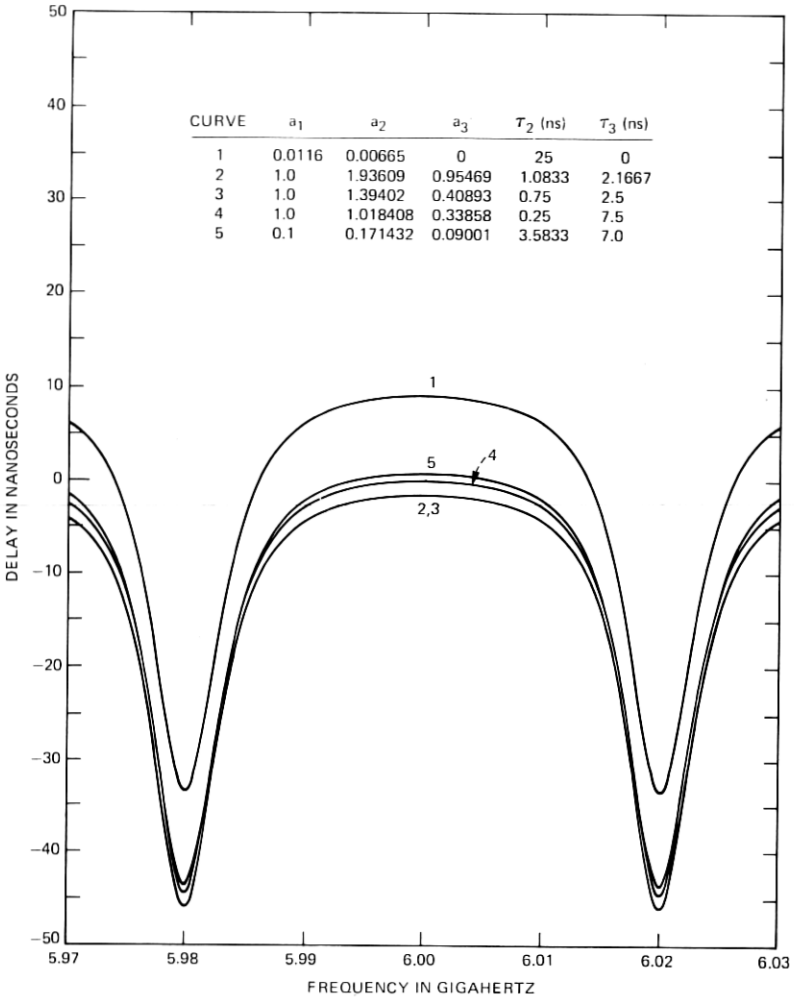

Fig. 5b—Delay distortion characteristics corresponding to the MTFs of Fig. 5a.

(10) may be used to calculate the attenuation and delay characteristics of the other MTFs in Fig. 5, and the nature of the zeros may be determined by noting whether the delay distortion is experiencing a minimum or maximum near each transmission minimum. By this means, we find that the fourth MTF has right-half-plane zeros near frequencies of $(3.333 + 4k)$ GHz, $k = 0, 1, 2, \cdots, \infty$. The fifth MTF is periodic in 12 GHz, with 84 zeros in each period. Adjacent zeros alternate between the left and right half planes except for the pair closest to 6 GHz which are both left-half-plane zeros (see Fig. 5) and the two closest to 12 GHz, which are both right-half-plane zeros.

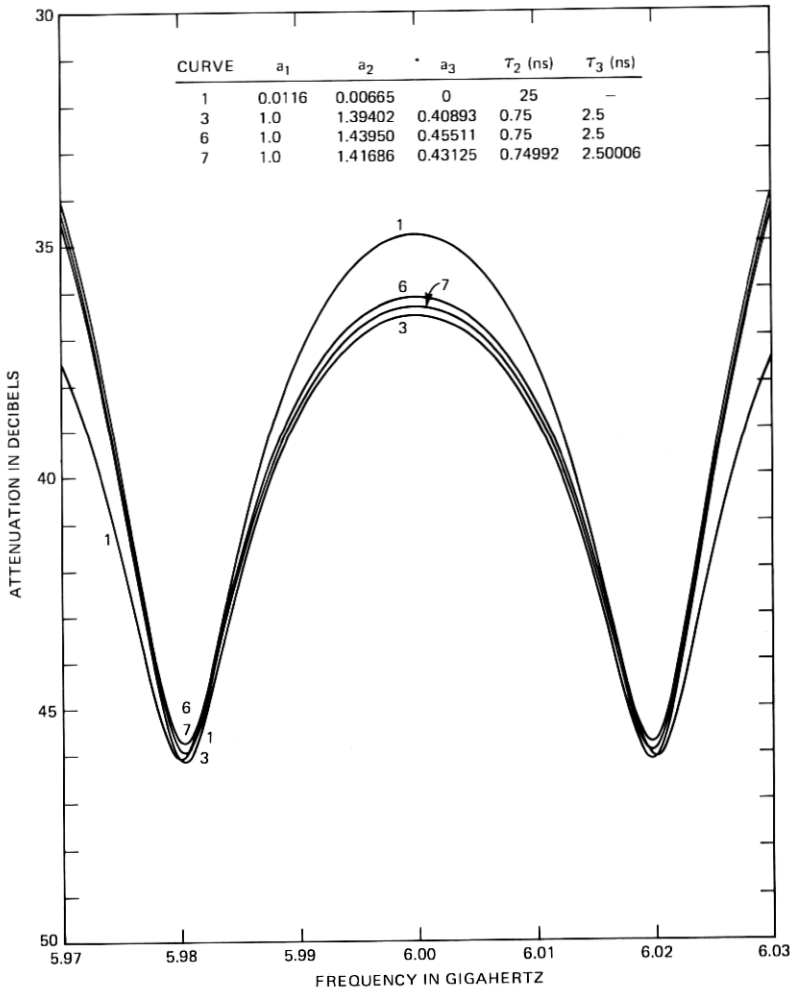

Fig. 6a—Attenuation characteristics of two-path (curve 1) and three-path MTFs with transmission minima at 5980 and 6020 MHz. The associated zeros of the transfer functions for curves 1 and 3 are both in the left half plane, and for curve 6 are both in the right half plane. For curve 7, the lower frequency one is in the left half plane and the other in the right half plane.

Although verifying the statements of the preceding paragraph may be tedious, the conclusions are important. The envelope delay of an MTF can look like that of a minimum phase function even if the function is not minimum phase; conversely, one cannot determine whether an MTF is truly minimum phase by examining its amplitude and phase in a frequency band less than its period in the frequency domain [$1/\tau_0$ in eq. (29)]. Thus, as predicted in Section 2.2, we have demonstrated that the delay distortion characteristics of an MTF in a frequency band depend only on the nature of the local zeros.

CURVE	a_1	a_2	a_3	τ_2 (ns)	τ_3 (ns)
1	0.0116	0.00665	0	25	–
3	1.0	1.39402	0.40893	0.75	2.5
6	1.0	1.43950	0.45511	0.75	2.5
7	1.0	1.41686	0.43125	0.74992	2.50006

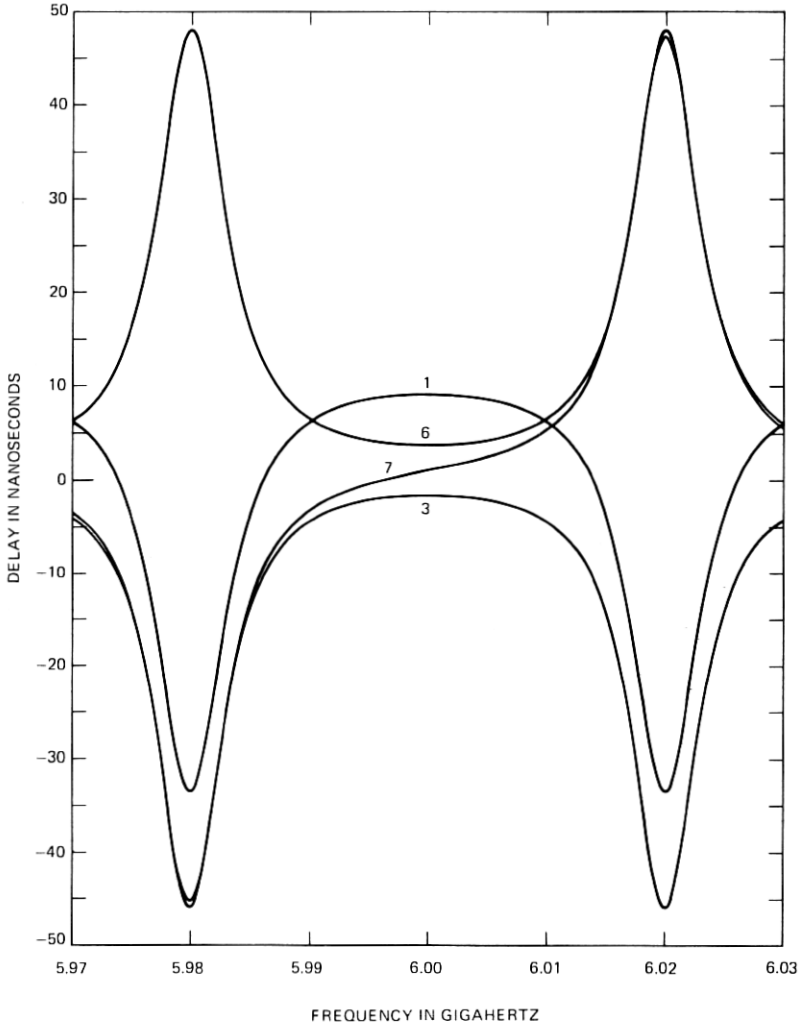

Fig. 6b—Delay distortion characteristics corresponding to the MTFs of Fig. 6a.

To demonstrate just how localized the delay characteristic is to the nature of the nearest zero, consider the effect of moving into the right half plane one or both of the zeros in the preceding example. Figure 6 compares the attenuation and delay characteristic for these cases [with $M_1 = 4$, $M_2 = 15$ in (52)]. It is apparent that neither zero impacts on the shape of the delay curve in the neighborhood of the other.

3.3 General synthesis problem

Consider the case where one wishes to construct an MTF that will have M zeros at specified complex frequencies. The most direct procedure is to extend the method described in Section 3.2 [eqs. (49) to (53)]. This procedure leads to an MTF with $M + 1$ paths; it requires M equations of the form of eq. (52) and M complex equations, or $2M$ real equations of the form of eq. (53). The only uncertainty with this method is the initial choice of the θ_i's; there is no apparent geometric construct at an appropriately defined mid-frequency that will instruct one in a good initial choice for the iterative procedure. No attempts have been made to apply this procedure to the case of M zeros. A simpler procedure that uses a greater number of delays is described in the following paragraphs.

One may synthesize an MTF capable of matching M zeros by assuming that the associated z-plane polynomial is of the form

$$P(z) = \prod_{m=1}^{M} (a_m + z^{n_m}), \tag{55}$$

where the a_m are all positive real numbers and the n_m are integers. Such a model leads to an MTF with 2^M delay paths. We note that the mth factor in (55) has its z-plane zeros uniformly spaced on a circle of the radius $|(a_m)^{1/n_m}|$. Thus, the kth zero of the mth term, which we denote as the k_mth zero, is at

$$z_{mk} = |(a_m)^{1/n_m}| e^{-j\frac{2k-1}{n_m}\pi} \qquad \begin{matrix} m = 1, 2, \cdots, M \\ k = 1, 2, \cdots, n_m. \end{matrix} \tag{56}$$

We achieve a synthesis by requiring the k_mth zero in the z-plane to map the mth zero in the s-plane. Denoting the mth s-plane zero by $\sigma_m + j\omega_m$ and using the transformation of eq. (29) with (56), we find

$$a_m = e^{-\sigma_m n_m \tau_0} \tag{57}$$

$$n_m \tau_0 = \frac{2k_m - 1}{2f_m}. \tag{58}$$

Thus, for a set of M integers $\{k_m\}$, one may determine the set of delays $\{n_m\tau_0\}$ through (58), and the coefficients a_m through (57). Used in conjunction with eqs. (55) and (29), these are sufficient to determine $H(j\omega)$. Note that the maximum delay is $\sum_m n_m \tau_0$.

Although knowledge of τ_0 is not necessary to the development, it can be shown that

$$\tau_0 = \frac{[\text{lcm}\{f_m\}]^{M-1}}{2\prod_{m=1}^{M} f_m}, \tag{59}$$

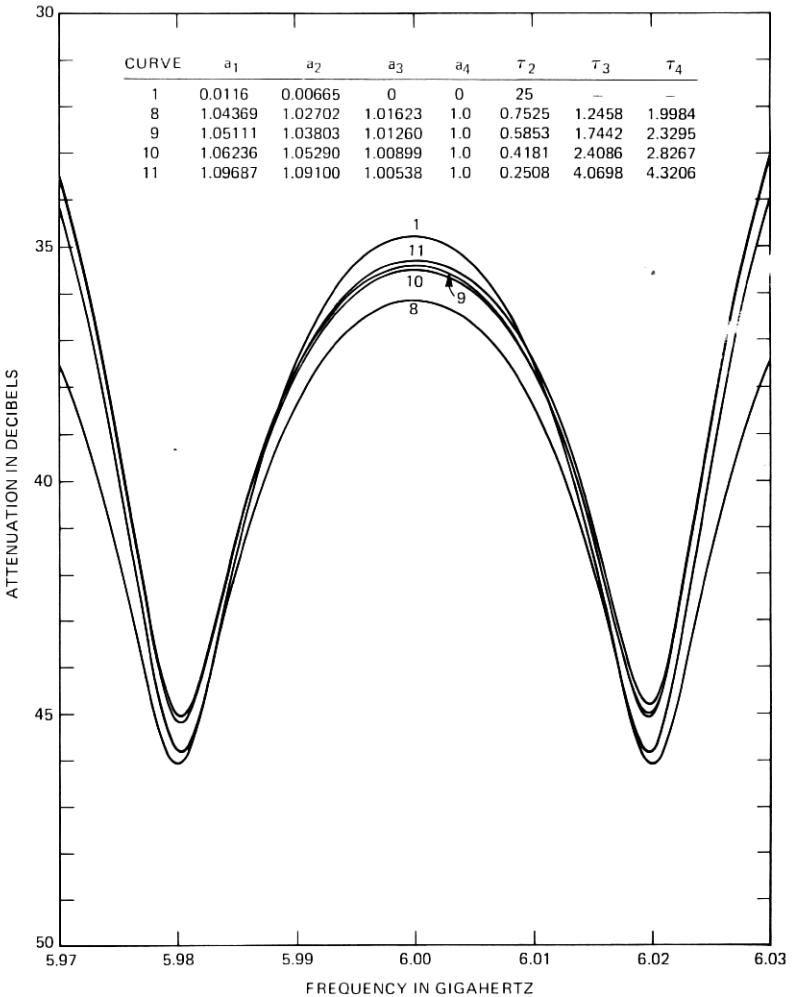

Fig. 7a—Attenuation characteristics of two-path (curve 1) and four-path MTFs with transmission minima at 5980 and 6020 MHz. The transfer function zeros associated with these minima are in the left half plane.

where lcm$\{f_m\}$ is the least common multiple of the set of frequencies $\{f_m\}$.

Figure 7 shows the attenuation and envelope delay of four different MTFs generated by this method to match the same zero locations as the preceding three-path example. The attenuation and delay of the two-path MTF of (54) are also shown. All four functions shown are minimum-phase everywhere. Figure 8 is similar to Fig. 6 in that it shows the effect on the four-path MTFs of shifting one or both zeros to the right half plane. The similarity between Figs. 6 and 8 is striking. It

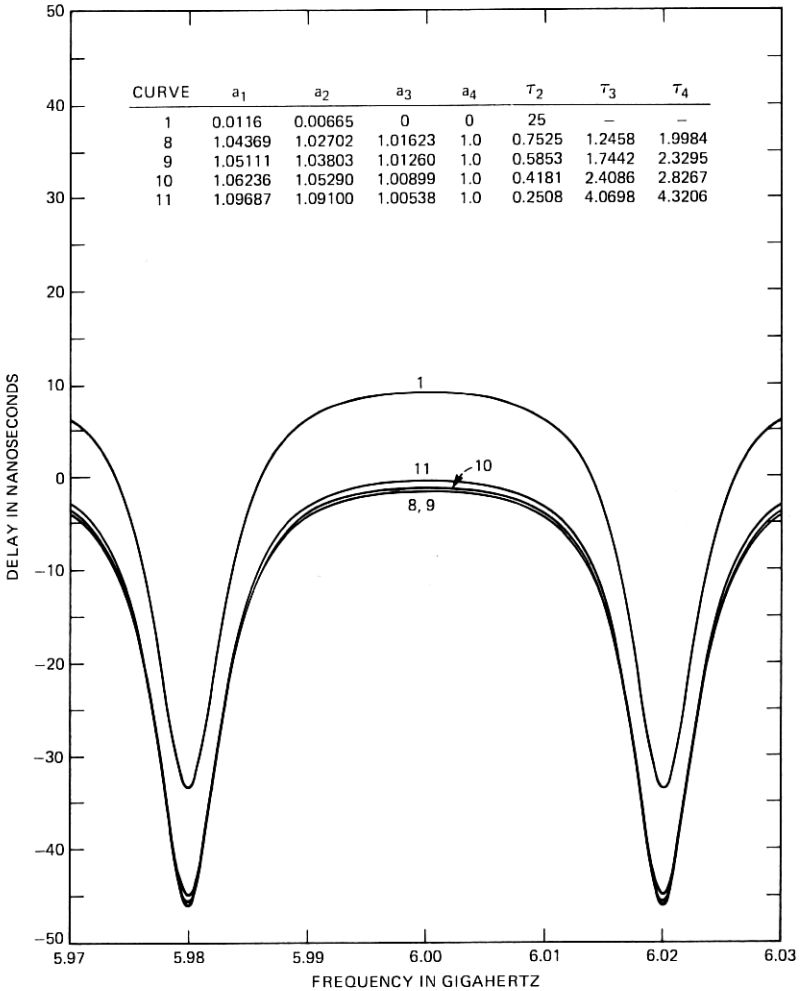

Fig. 7b—Delay distortion characteristics corresponding to the MTFs of Fig. 7a.

is noteworthy that all the MTFs shown in Figs. 7 and 8 have path strengths that are close to unity. Such solutions are typical for this synthesis method; in accepting 2^M delays for matching M zeros, we obtain 2^M path strengths that are close to unity for $|\sigma_m|$ sufficiently small.

IV. MODELING MULTIPATH TRANSFER FUNCTIONS

The evaluation of the performance of radio systems in the common carrier bands requires a statistical model of the channel. The required model is essentially a channel transfer function with parameters whose

values are determined from statistical distributions. Using the parameter statistics, one can determine the probability of finding a channel transfer function corresponding to a given element of parameter space. Equivalently, one can determine the fraction of time that the channel condition will exceed some measured bound. The concerns of the general modeling problem include: choosing parameters to measure, determining sample spacings in time and frequency, evaluating the effects of measurement noise and quantization, and estimating model

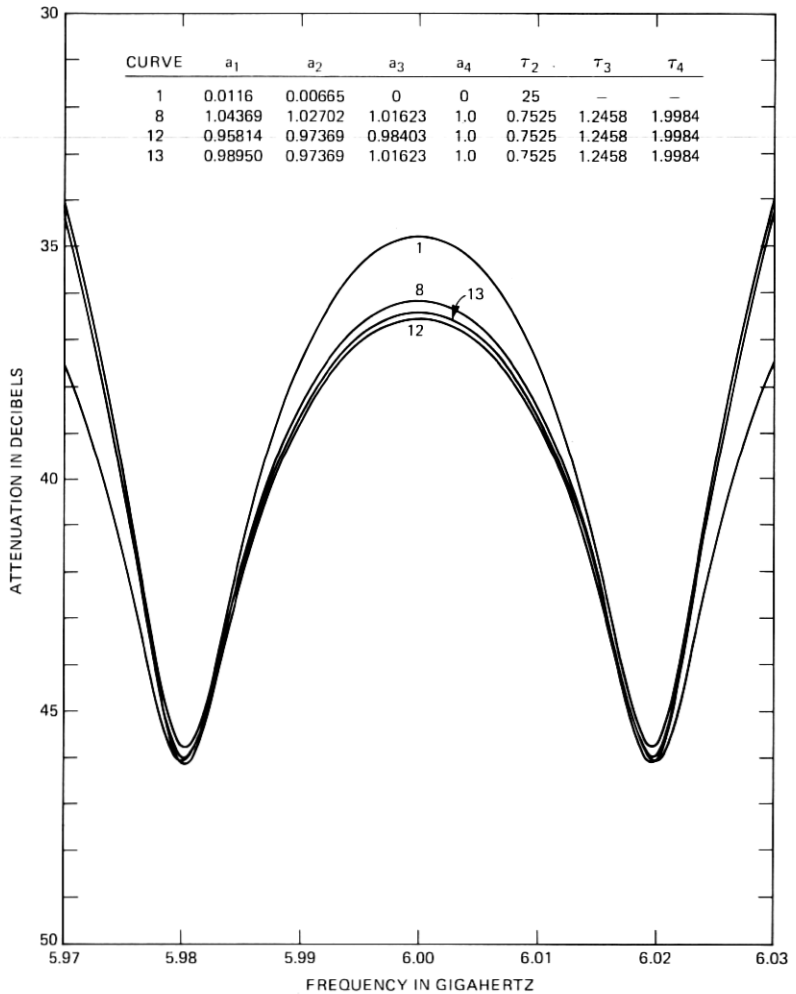

Fig. 8a—Attenuation characteristics of two-path (curve 1) and four-path MTFs with transmission minima at 5980 and 6020 MHz. The associated zeros of the transfer functions for curves 1 and 8 are both in the left half plane, and for curve 12 are both in the right half plane. For curve 13, the lower frequency one is in the left half plane and the other in the right half plane.

CURVE	a_1	a_2	a_3	a_4	τ_2	τ_3	τ_4
1	0.0116	0.00665	0	0	25	–	–
8	1.04369	1.02702	1.01623	1.0	0.7525	1.2458	1.9984
12	0.95814	0.97369	0.98403	1.0	0.7525	1.2458	1.9984
13	0.98950	0.97369	1.01623	1.0	0.7525	1.2458	1.9984

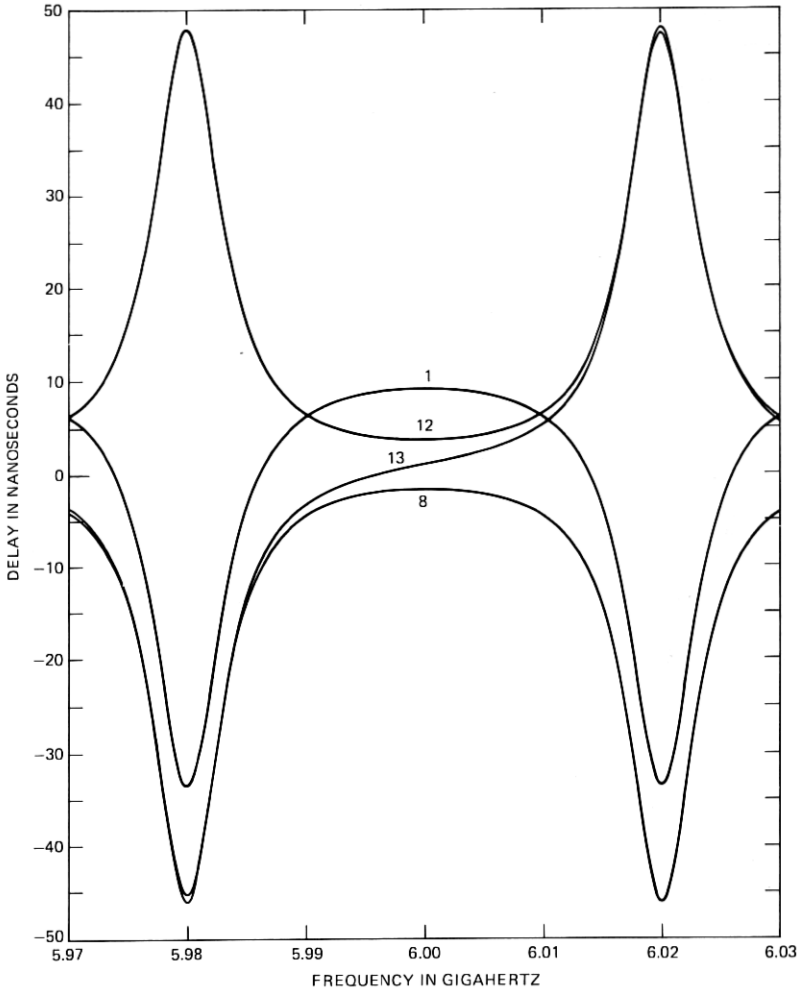

Fig. 8b—Delay distortion characteristics corresponding to the MTFs of Fig. 8a.

parameters from the observed data. In this section, we limit our discussions to part of the underlying modeling problem which may be more accurately described as the approximation problem. Thus, our concern is to determine, given perfect and complete data, how we can best describe what has been observed.

Since the maximum delays observable in typical microwave radio hops are on the order of 10 ns, the average frequency spacing of the

zeros of channel transfer functions is about 100 MHz, as discussed in Section 2.4. This spacing is large compared to the channel bandwidths of 20 to 40 MHz in the common carrier bands. On the average, we expect the channel transfer function to be influenced by only one zero; however, observations[4] suggest that spacings as small as 40 MHz may be observed for 40 seconds a month. Although multiple zeros in band are observed occasionally, it is probably not necessary to have a model capable of representing such a situation because of the infrequency and short duration of such events. In brief, one would use a more complicated model only if it more accurately represented the channel for a greater fraction of the fading time, and if this incremental improvement had a significant impact on equipment performance estimates. Thus, as a minimum, a channel model should be capable of representing the channel transfer function when there is one zero in or near the channel. However, to accurately predict outage for radio systems with very effective equalizers might require a model capable of representing a channel when a second zero is nearby. We shall consider below two model alternatives for both the single zero case and the double zero case.

In Section 3.2 we demonstrated that knowledge of the precise location of two moderately closely spaced zeros was sufficient to determine the transmission characteristics in the frequency band near those zeros, but was not sufficient to uniquely determine the five parameters of a three-path fade. From this it follows that a multipath model should not require more than four parameters; i.e., eq. (47) should be sufficient. On the other hand, since only a finite number of zeros have impact on the transfer function and a complex function in the neighborhood of its zeros is well represented by a power series expansion, one can use a model based on a power series expansion of the transfer function.

4.1 Channel transfer function dominated by a single zero

Let us first consider the case where the channel transfer function may be characterized, in a frequency band, by a single term in the product expansion of eq. (13). It is equivalent to use a group of terms, or a single term of the expansion of eq. (32). This results in the simple three-path model described in Section 3.1, with response given by:

$$H(j\omega) = a[1 - be^{-j(\omega-\omega_0)\tau_0}]. \tag{47}$$

If the channel, of width f_B, is under the influence of a single zero, one may fix the value of τ_0, at any value less than $1/(6f_B)$, and use eq. (47) as a three-parameter model. Although the fixed-delay model fits the observed channel characteristics equally well regardless of the particular choice of τ_0, the statistics of the remaining parameters do depend

on the choice. A 6-GHz channel has been successfully characterized with such a model.[4,5]

If one takes, as a channel model, a single term from eq. (13) and ignores the residual exponential terms, one obtains

$$H(j\omega) = a[\sigma_1 - j(\omega_c - \omega_1) - j(\omega - \omega_c)]. \tag{60}$$

For the model function, we have chosen the zero at $j\omega_1 + \sigma_1$ and shown the function as expanded about a convenient frequency, ω_c. The factor a represents the composite effect of all other terms in the expansion of eq. (13). This model has been proposed and used for channel modeling.[3,20,21] Although the modeled function of eq. (60) does not represent the response of a real physical network, it can be approximated by standard bandpass techniques.

It is apparent that the model of eq. (60) and the fixed delay model of eq. (47) are both three-parameter models that are representing the same phenomena in the same manner. Given that only one dominant zero is affecting the channel transfer function, there is little difference between the accuracy with which these two models can represent the state of the channel.

4.2 Channel transfer function with one dominant zero and second zero nearby

Assume that a second zero, more distant from the band center than the primary zero, is exerting an influence on channel attenuation and delay distortion. From discussions in conjunction with eqs. (17) and (18) and from examples in Section 3.3, we expect the second zero to evidence itself primarily through the shape of the attenuation characteristics, which may exhibit both a maximum and a minimum in band.

With the simple three-path model of eq. (47), this situation may be accommodated by allowing the delay τ_0 to be variable. Thus, the delay is increased to the point where an adjacent zero is brought close enough to produce the desired effect.

With a power series model, this situation may be accommodated by introducing additional terms from eq. (13). By analogy with eq. (60), we assume a model of the form

$$\begin{aligned} H(j\omega) &= a[\sigma_1 - j(\omega_c - \omega_1) - j(\omega - \omega_c)] \\ &\quad \cdot[\sigma_2 - j(\omega_c - \omega_2) - j(\omega - \omega_c)] \\ &= a\{[\sigma_1\sigma_2 - (\omega_c - \omega_1)(\omega_c - \omega_2)] \\ &\quad - j[\sigma_2(\omega_c - \omega_1) + \sigma_1(\omega_c - \omega_2)] \\ &\quad - [2\omega_c - \omega_1 - \omega_2][\omega - \omega_c] \\ &\quad - j[\sigma_1 + \sigma_2][\omega - \omega_c] - [\omega - \omega_c]^2\}. \end{aligned} \tag{61}$$

We see that the five-parameter, power series model of eq. (61) is more flexible than the four-parameter delay model because it can place the second zero arbitrarily, whereas the delay model has all zeros at the same σ value.

If, for the power series model, we force $\sigma_2 = -\sigma_1$ it reduces to a four-parameter model. This four-parameter model is comparable to the simple three-path model; however, the two models cannot be made to match each other exactly because of their structural properties. The zeros of the simple three-path model are members of an infinite equally spaced set; hence, its attenuation characteristics will have symmetric maxima (transmission minima). Since the power series model has only two zeros, its attenuation maxima will be asymmetric (as are the cases shown in Fig. 5, which have no other zero nearby).

We conclude that there would be only slight differences between the characteristics that can be generated by the simple three-path model and a four-parameter, power series model. Thus, the choice between power series and delay models for channel characterization is more likely to depend on the convenience of using the model and its parameter statistics in verifying the performance of radio systems by theoretical calculation or by laboratory measurement.

V. SUMMARY AND CONCLUSIONS

The primary accomplishment of this study is to provide the basis for relating the observed transmission characteristics of a narrowband channel (in terms of attenuation and envelope delay distortion functions*) to the physical parameters (in terms of path delays and amplitudes) which give rise to multipath fading. The interrelations were obtained by using the well-known property of pure delay networks: that they may be uniquely represented in terms of their s-plane zeros.

We have shown that the attenuation and delay characteristics of a multipath transfer function can each be expressed as a summation of primary attenuation and delay functions. Except for changes and shifts in scale, all those primary functions, of a given type, are identical, and each represents the effect of a single zero. Thus, one can relate the attenuation or delay characteristics to the positions of the zeros and hence to each other.† (The transmission characteristic of a radio channel in the common carrier bands is usually dominated by a single zero during periods of multipath fading.)

We have shown that the average spacing of the zeros along the

* A novel and simple means of relating the delay distortion to the network transfer function is derived. This relation may be particularly useful for network designers.

† There is ambiguity because the delay distortion of a minimum phase (left-half-plane) zero is the negative of that of a nonminimum phase (right-half-plane) zero.

frequency axis is the reciprocal of the longest physical delay difference present in the channel. Since each zero will cause (at most) a single maximum in the attenuation characteristic, one can estimate the maximum observable delay by determining the average frequency spacing of the attenuation maxima. Using an argument that the zeros show no statistical preference for any particular frequency, one can estimate the spacing from a sequence of observations in a narrow frequency band.* All available measurements in the frequency domain suggest a delay of about 10 ns for the average value of the largest delay spread present in a microwave line-of-sight radio path of 22- to 30-mile length. This estimate is in reasonable agreement with short pulse measurements and theoretical estimates for the same paths.

While a given delay network with N paths and a total delay spread of 10 ns would have zeros with an average spacing of 100 MHz, there is no minimum spacing between zeros; that is, two zeros may be arbitrarily close to each other. Several synthesis procedures were developed to match multipath transfer functions at several complex zeros. For instance, one can find about 1800 three-path delay networks with delay spreads less than 10 ns that will match at zeros 40 MHz apart near 6 GHz. A similarly sized family of four-path networks can be developed. The point of these exercises is to demonstrate that one can construct large families of multipath delay functions with widely differing delays but all with approximately the same attenuation and delay distortion functions over wide bandwidths (60 MHz for the example chosen). In other words, the shape of the attenuation and delay distortion curves over a 60-MHz bandwidth gives no information as to the spread of physical delays that might be present in the channel. Alternatively, one cannot construct a unique delay network from information obtained in a finite frequency band.

The material presented in the final section demonstrates that there is virtually no difference in the modeling capability of a three-parameter (fixed-delay) multipath model and a three-parameter power-series model. The differences between a four-parameter delay model and a four-parameter power-series model are also of little significance. Although the four-parameter models have more flexibility than three-parameter models, it is not clear that such flexibility is required for evaluating any existing or projected radio system. It appears that more significant differences between delay and power-series models could exist in the following areas: (*i*) the ease with which model parameters may be estimated from available field data; (*ii*) the convenience in representing the joint statistics of the model parameters; and (*iii*) the facility with which the statistical models may be used to calculate and measure the performance of digital systems.

* This argument is similar to the ergodic hypothesis.

VI. ACKNOWLEDGMENT

The author is indebted to his colleagues in the Radio Analysis Group for many fruitful discussions of various aspects of the work reported here. W. T. Barnett provided invaluable insights into the phenomenology of multipath fading in general and comments on this manuscript in particular. The assistance of M. V. Pursley in generating the computer-drawn plots is gratefully acknowledged.

APPENDIX

In this appendix, we determine the conditions under which two simple three-path fades have matching amplitude and envelope delay characteristics over a frequency band f_B either side of the frequency where they both have a minimum. Using eq. (47), the two transfer characteristics are given by

$$H_1(\omega) = a_1(1 - b_1 e^{-j\omega\tau_1}) \tag{62}$$

$$H_2(\omega) = a_2(1 - b_2 e^{-j\omega\tau_2}), \tag{63}$$

where, without loss of generality, we have set $\omega_0 = 0$. We assume that the magnitudes and the second derivatives of the magnitudes of these functions are matched at $\omega = 0$. This gives

$$a_1(1 - b_1) = (1 - b_2)a_2 \qquad 0 < a_2 \leq a_1 \leq 1 \tag{64}$$

and

$$\frac{\sqrt{b_1}\tau_1}{1 - b_1} = \frac{\sqrt{b_2}\tau_2}{1 - b_2} = \alpha. \tag{65}$$

The ratio of the magnitude squared of the two responses is given by

$$R(\omega) = \frac{|H_1(\omega)|^2}{|H_2(\omega)|^2} = \frac{1 + g_1}{1 + g_2}, \tag{66}$$

where

$$g_1 = \left(\alpha\omega \operatorname{sinc} \frac{\omega\tau_1}{2}\right)^2 \tag{67}$$

$$g_2 = \left(\alpha\omega \operatorname{sinc} \frac{\omega\tau_2}{2}\right)^2 \tag{68}$$

$$\operatorname{sinc} x = \frac{\sin x}{x}. \tag{69}$$

From (64) we know that

$$b_1 \geq b_2, \tag{70}$$

and hence from (65) that

$$\tau_2 \geq \tau_1. \tag{71}$$

By definition, then,

$$\operatorname{sinc} \frac{\omega\tau_1}{2} \geq \operatorname{sinc} \frac{\dot{\omega}\tau_2}{2} \qquad |\omega\tau_2| < \pi. \tag{72}$$

It follows that

$$1 \leq R(\omega) \leq \left(\frac{\operatorname{sinc}(\omega\tau_1/2)}{\operatorname{sinc}(\omega\tau_2/2)}\right)^2 \leq \frac{1}{[\operatorname{sinc}(\omega\tau_2/2)]^2} \tag{73}$$

or

$$1 \leq R(\omega) \leq \frac{1}{1 - [(\omega\tau_2)^2/12]}, \tag{74}$$

where we have used the relation

$$\operatorname{sinc}^2 x = \frac{1}{2x^2}[1 - \cos 2x] = 1 - \frac{x^2}{3} + \frac{2x^4}{45} - \cdots. \tag{75}$$

If we impose the condition $|\omega\tau_2| \leq \pi/3$, we find

$$1 \leq R(\omega) \leq \frac{1}{1 - (\pi^2/108)} \approx 1.106. \tag{76}$$

Hence, the amplitude characteristics track to within 0.4 dB for $\omega\tau_2 \leq \pi/3$. For a 25-mHz bandwidth with the minimum at one edge, this condition corresponds to $\tau_2 \leq 1/6B \approx 6.7$ ns.

By comparison with eqs. (42) and (44), we may write the expression for the envelope delay distortion of (62) and (63), relative to the distortion at $\omega = 0$, as

$$\delta\phi_1 = \frac{2b_1\tau_1(1 + b_1)\sin^2 \omega\tau_1/2}{(1 - b_1)[(1 - b_1)^2 + 4b_1 \sin^2 \omega\tau_1/2]} \tag{77}$$

and

$$\delta\phi_2 = \frac{2b_2\tau_2(1 + b_2)\sin^2 \omega\tau_2/2}{(1 - b_2)[(1 - b_2)^2 + 4b_2 \sin^2 \omega\tau_2/2]}. \tag{78}$$

The fractional error between these is denoted by Φ where

$$\Phi = \frac{\delta\phi_2 - \delta\phi_1}{\delta\phi_1}. \tag{79}$$

From (77) and (78),

$$\frac{\delta\phi_2}{\delta\phi_1} = \frac{\tau_2(1 + b_2)}{(1 - b_2)} \cdot \frac{(1 - b_1)}{\tau_1(1 + b_1)} \frac{g_2}{1 + g_2} \cdot \frac{1 + g_1}{g_1}. \tag{80}$$

Using (65), this becomes

$$\frac{\delta\phi_2}{\delta\phi_1} = \frac{(\sqrt{b_2} + 1/\sqrt{b_2})}{(\sqrt{b_1} + 1/\sqrt{b_1})}\left(\frac{1 + 1/g_1}{1 + 1/g_2}\right). \tag{81}$$

From (67), (68), and (72),

$$\frac{g_2}{g_1} = \frac{\operatorname{sinc}^2(\omega\tau_2/2)}{\operatorname{sinc}^2(\omega\tau_1/2)} \leq 1. \tag{82}$$

It follows from this and from (73) and (74) that

$$1 - \frac{(\omega\tau_2)^2}{12} \leq \frac{g_2}{g_1} \leq \frac{1 + 1/g_1}{1 + 1/g_2} \leq 1. \tag{83}$$

Since $\sqrt{x} + 1/\sqrt{x}$ is an increasing function of $|1 - x|$, it follows from (70) that

$$\frac{\sqrt{b_2} + 1/\sqrt{b_2}}{\sqrt{b_1} + 1/\sqrt{b_1}} \geq 1. \tag{84}$$

It is easily shown that for $x < 1$

$$2 \leq \sqrt{1 - x} + \frac{1}{\sqrt{1 - x}} \leq 2 + \frac{x^2}{4(1 - x)}. \tag{85}$$

From this, we see that

$$\frac{\sqrt{b_2} + 1/\sqrt{b_2}}{\sqrt{b_1} + 1/\sqrt{b_1}} \leq 1 + \frac{(1 - b_2)^2}{8b_2}. \tag{86}$$

Using (83), (84), and (86) in (81) gives

$$1 - \frac{(\omega\tau_2)^2}{12} \leq \frac{\delta\phi_2}{\delta\phi_1} \leq 1 + \frac{(1 - b_2)^2}{8b_2}. \tag{87}$$

Substituting in (79) gives the bound on the fractional error as

$$-\frac{(\omega\tau_2)^2}{12} \leq \Phi \leq \frac{(1 - b_2)^2}{8b_2}. \tag{88}$$

The condition $|\omega\tau_2| \leq \pi/3$ was chosen to keep the inband amplitude error to less than 0.5 dB [see (76)]. Applying this same condition to (88) gives $\Phi \geq -0.091$. If we limit values to b_2 such that

$$0.436 \leq b_2 \leq b_1,$$

then

$$-0.091 \leq \Phi \leq 0.091$$

or

$$|\Phi| \leq 0.091.$$

REFERENCES

1. W. D. Rummler, "A Multipath Channel Model for Line-of-Sight Digital Radio Systems," International Conference on Communications 1978, Conference Record Vol. 3 (June 1978), pp. 47.5.1–4.
2. V. K. Prabhu and L. J. Greenstein, "Analysis of Multipath Outage with Applications to 90 Mb/s PSK Systems at 6 and 11 GHz," International Conference on Communications 1978, Conference Record Vol. *3* (June 1978), pp. 47.2.1–5.
3. L. J. Greenstein, "A Multipath Fading Channel Model for Terrestrial Digital Radio," IEEE Trans. Commun., *COM-26*, No. 8 (August 1978), pp. 1247–1250.
4. W. D. Rummler, "A New Selective Fading Model: Application to Propagation Data," B.S.T.J., *58*, No. 7 (May–June 1979), pp. 1037–1071.
5. C. W. Lundgren and W. D. Rummler, "Digital Radio Outage Due to Selective Fading—Observation vs Prediction From Laboratory Simulation," B.S.T.J., *58*, No. 7 (May–June 1979), pp. 1073–1100.
6. C. L. Ruthroff, "Multi-Path Fading on Line-of-Sight Microwave Radio Systems as a Function of Path Length and Frequency," B.S.T.J., *50*, No. 7 (September 1971), pp. 2375–2398.
7. O. E. DeLange, "Propagation Studies at Microwave Frequencies by Means of Very Short Pulses," B.S.T.J., *31*, No. 1 (January 1952), pp. 91–103.
8. A. B. Crawford and W. C. Jakes, Jr., "Selective Fading of Microwaves," B.S.T.J., *31*, No. 1 (January 1952), pp. 68–90.
9. R. L. Kaylor, "A Statistical Study of Selective Fading of Super-High Frequency Radio Signals," B.S.T.J., *32*, No. 9 (September 1953), pp. 1187–1202.
10. P. Bello, L. W. Pickering, and C. J. Boardman, "Multipath over LOS Channels Study," CNR, Inc. Final Technical Report for Rome Air Development Center, November 1977 (RADC-TR-77-355).
11. W. C. Jakes, Jr., "An Approximate Method to Estimate an Upper Bound on the Effect of Multipath Delay Distortion on Digital Transmission," IEEE Trans. Commun., *COM-27*, No. 1 (January 1979), pp. 76–81.
12. E. A. Guillemin, *Theory of Linear Physical Systems*, New York: John Wiley, 1963.
13. E. A. Guillemin, *Synthesis of Passive Networks*, New York: John Wiley, 1957.
14. P. M. Morse and H. Feshbach, *Methods of Theoretical Physics*, Part I, New York: McGraw-Hill, 1953.
15. E. Goursat, *A Course in Mathematical Analysis, Vol. II. Part I, Functions of a Complex Variable*, New York: Dover, 1959.
16. H. Bohr, *Almost Periodic Functions*, New York: Chelsea, 1951.
17. A. S. Besicovitch, *Almost Periodic Functions*, New York: Dover, 1954.
18. B. Ja. Levin, *Distribution of Zeros of Entire Functions*, Appendix VI. Providence, R.I.: American Mathematical Society, 1964.
19. G. M. Babler, "Measurements of Delay Distortion During Selective Fading," International Conference on Communications 1974, Conference Record, (June 1974), pp. 12A.1–4.
20. L. J. Greenstein and B. Czekaj, "A Statistical Power Series Model for Multipath Fading Channel Responses," International Conference on Communications 1979, Conference Record, Vol. *2*, (June, 1979), pp. 23.1.1–5.
21. L. J. Greenstein and B. Czekaj, "A Polynomial Model for Multipath Fading Channel Responses," B.S.T.J., *59*, No. 7 (September 1980).